Rare Metal Materials and Engineering
Volume 51, Issue 10, October 2022
Available online at www.rmme.ac.cn

Science Press

Cite this article as: Zhang Yijie, Du Jinghong, Ji Quanxin, et al. Effect of Sr and Y Addition on Microstructure and Mechanical Properties of A356 Aluminum Alloy and Its Mechanism[J]. Rare Metal Materials and Engineering, 2022, 51(10): 3588-3595.

ARTICLE

Effect of Sr and Y Addition on Microstructure and Mechanical Properties of A356 Aluminum Alloy and Its Mechanism

Zhang Yijie[1], Du Jinghong[1], Ji Quanxin[1], Sun Yanhua[2], Feng Weiguang[2], Bao Chongjun[2], Li Yuzhang[2], Yan Jikang[3]

[1] Faculty of Materials Science and Engineering, Kunming University of Science and Technology, Kunming 650093, China; [2] Kunming Metallurgical Research Institute Co., Ltd, Kunming 650031, China; [3] School of Engineering, Southwest Petroleum University, Nanchong 637001, China

Abstract: The effects of Sr and Y addition on the microstructure and mechanical properties of A356 aluminum alloy were studied by metallographic microscope, scanning electron microscope, transmission electron microscope, energy dispersive spectra and mechanical property tests. The results show that the combined addition of Sr and Y can obtain the best microstructure and mechanical properties compared with the separate addition of Sr or Y. The eutectic Si changes completely from flake-like or acicular-like to fibrous shape, the equivalent grain diameter of α-Al decreases from 42.49 μm to 26.63 μm, the secondary dendrite arms spacing (SDAS) decreases from 22.38 μm to 13.60 μm, the tensile strength increases from 166.1 MPa to 185.3 MPa, the elongation increases from 3.6% to 7.6%, and the fracture mode changes from brittle fracture to ductile-brittle fracture. The refinement mechanism and modification mechanism of Sr and Y were discussed. It is concluded that the main reason for α-Al grain refinement is the rapid heterogeneous nucleation of α-Al based on Al_3Y, and the modification mechanism is impurity-induced twins which grow in the mechanism of twin plane reentrant edge.

Key words: A356; grain refinement; the modification of eutectic Si; mismatch; twin

At present, A356 aluminum alloy is mainly used for aluminum alloy wheels produced by casting process. With the development of automobile industry, the machinability, safety and durability of wheels are constantly improved, leading to higher requirements for the performance of A356 aluminum alloy. A356 alloy is a hypoeutectic cast aluminum alloy of Al-Si-Mg system, which has the characteristics of good casting fluidity, good air tightness, low shrinkage and low hot cracking tendency[1, 2]. Due to the existence of coarse and irregularly shaped eutectic Si in unmodified A356, the aluminum alloy matrix is seriously split and the continuity of the aluminum matrix is destroyed, thus reducing the strength and plasticity of the alloy[3, 4]. Therefore, the modification of eutectic Si to improve the adverse effect of flake-like or acicular-like eutectic Si on the matrix is an important way to improve the mechanical properties of A356 aluminum alloy.

The common modification of A356 alloy is to improve the shape, size and distribution of silicon phase in the alloy by adding some elements. The common modifiers are Na, Ca, Sr, Ba, rare earth, etc, among which Sr has the best modification effect and is a long-term modifier[5-7]. Another important way to improve the mechanical properties of A356 aluminum alloy is to refine α-Al grains. The commonly used refiners are Al-Ti-B, Al-Ti-C, Zr, RE, etc. Rare earths can not only refine grains and modify eutectic Si in A356, but also refine, remove impurities and improve iron-rich phase. In addition, the modification of rare earth has relatively long-term effects and remelting stability[8,9]. So it is an excellent additive for cast

Received date: October 28, 2021
Foundation item: Major Science and Technology Project in Yunnan Province-New Material Special Project (202102AB080015, 202102AB080004, 2018ZE005, 2019ZE001)
Corresponding author: Du Jinghong, Ph. D., Professor, Key Laboratory of Advanced Materials of Yunnan Province, Faculty of Materials Sciences and Engineering, Kunming University of Science and Technology, Kunming 650093, P. R. China, E-mail: cldjh@sina.com

aluminum alloy at present.

The composite addition of refiners and modifiers to Al-Si alloys has been investigated for a long time. More and more studies have shown that[10-12] rare earths can play a good synergistic effect when combined with other modifiers or refiners. Liu[13] et al found that the increase of composition undercooling and the production of nano-precipitates inhibit the growth of eutectic Si during solidification by studying the effect of Gd and Zr on A356. Qiu[14] et al found that the composite addition of Sr and La can significantly refine the grain and modify the eutectic Si. Dong[15] et al have revealed that the addition of Sr and Y can increase the nucleation undercooling of α-Al, and then increase the nucleation rate of α-Al, refining the grains and modifying the eutectic Si. In this work, strontium (Sr) and yttrium (Y) were selected as additive elements, since the atomic radius ratios of Sr to Si and Y to Si are close to the optimum atomic radius ratio of 1.6475 of impurity induced twins[16]. The effect of Sr and Y addition on the microstructure and properties of A356 and its mechanism were studied by microscopic analysis and mechanical properties test.

1 Experiment

The raw materials of the experiment were A356 aluminum alloy, Al-10Sr master alloy and Al-10Y master alloy. The composition of them is shown in Table 1. Four groups of alloys with different components were prepared, as shown in Table 2. Firstly, the addition amount of the material to be melted was calculated, and the weighed A356 aluminum alloy was put into a graphite crucible and heated to 750 °C in a resistance furnace. After the alloy was completely melted, the melt was degassed and the slag was removed with refining agent, and then the prepared master alloys were pressed into the bottom of the liquid aluminum with a bell cover. After the master alloy was melted, a covering agent was sprinkled to prevent the absorption of the molten aluminum during the heat preservation process. After holding at 750 °C for 20 min, manually stir for 5 min to homogenize the alloy elements. Finally, the temperature in the furnace was reduced to 720 °C, the slag was removed, and the liquid metal was poured into the metal mold at the preheating temperature of 300 °C to make a cylindrical aluminum ingot with Φ=15 mm and h=200 mm.

Table 1 Chemical composition of A356, Al-10Sr and Al-10Y master alloy (wt%)

Alloy	Si	Mg	Sr	Y	Impurity	Al
A356	6.94	0.36	-	-		
Al-10Sr	-	-	9.46	-	≤1	Bal.
Al-10Y	-	-	-	9.83		

Table 2 Composition of each sample (wt%)

Sample	Composition
A1	A356
A2	A356+0.04Sr
A3	A356+0.3Y
A4	A356+0.04Sr+0.15Y

Samples were taken in the middle of aluminum ingot by a cutting machine. After rough grinding, fine grinding and polishing, the surface of the samples was corroded with 0.5% HF solution, and the samples were deeply corroded with 35% HCl solution, and finally cleaned with alcohol and dried. The microstructure and morphology were observed by TX-400V optical microscope (OM), JSM-6490LV scanning electron microscope (SEM) and JEM-2100 transmission electron microscope (TEM). The tensile strength and elongation were tested by WAW-300 universal tensile testing machine, and the tensile rate was 3 mm/min. The DSC curves of each group of samples were measured by Mettler1600LF synchronous thermal analyzer. The protective gas was Ar gas, and the cooling rate was 5 °C/min.

2 Results and Discussion

2.1 Grain shape and size of α-Al

Fig. 1 shows the as-cast microstructures of A356 with different components. It can be seen that the optical structures of the four groups of A356 aluminum alloys added with different elements are obviously different. There are coarse α-Al dendrites in A1 sample, as shown in Fig. 1a, eutectic Si structures are stacked together and there is no obvious boundary with α-Al. When Sr is added, the size of α-Al hardly changes, and there are still obvious secondary dendrites, but there is a clear boundary between α-Al matrix and eutectic Si (Fig. 1b), which indicates that the effect of adding Sr alone cannot refine α-Al matrix. The grain size, number and spacing of secondary dendrites of α -Al are greatly reduced after adding Y element, as shown in Fig. 1c. After adding Sr and Y together, there is almost no secondary dendrite, and it shows a certain orientation of primary crystal. The shape and size of α-Al become uniform and the grains are mainly fine and dense equiaxed crystals, as shown in Fig.1d.

The equivalent grain diameter of α-Al was measured by the image analysis software Image-ProPlus6.0, and the SDAS was measured and calculated by the sectional line method and the formula below[17], respectively.

$$d = \frac{1}{m}\sum_{i=1}^{k}\left(\frac{l_i}{n_i - 1}\right) \quad (1)$$

where d is the SDAS; l_i is the total length of the line segment; n_i is the number of secondary dendrite arms crossed by the line segment; m is the number of measured line segments, and both ends of the line segments are located on the central axis of the secondary dendrite arm. The results are shown in Fig. 2 and Fig.3.

It can be seen that the equivalent grain diameter of sample A1 is about 42.49 μm and the SDAS value is about 22.38 μm. After adding Sr element, the equivalent grain diameter of α-Al changes little, which is about 43.29 μm, while SDAS decreases slightly, which is 19.85 μm. The equivalent grain diameter of α-Al is 28.97 μm and SDAS value is 14.59 μm

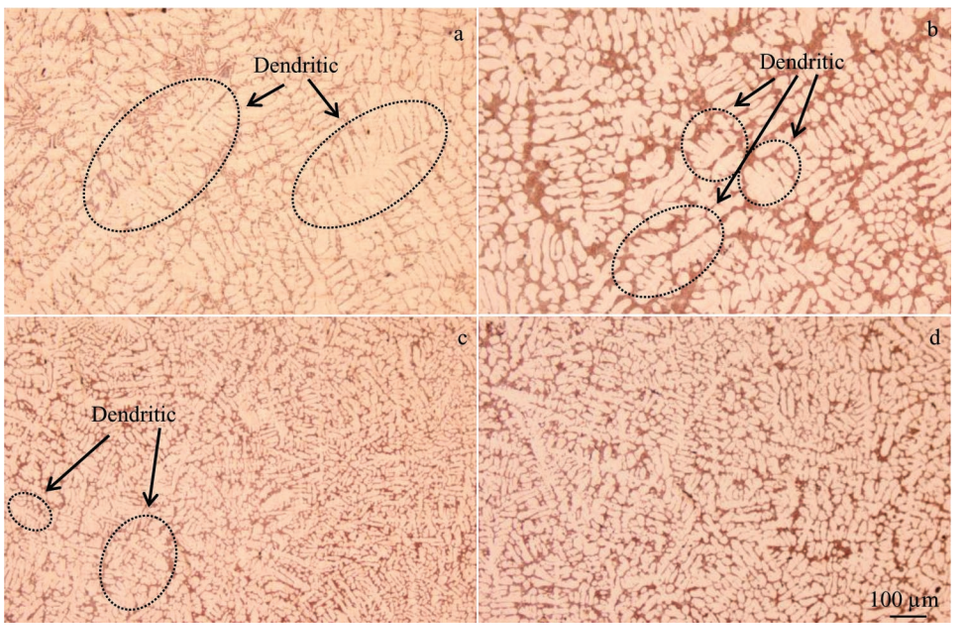

Fig.1 OM microstructures of A1 (a), A2 (b), A3 (c), A4 (d) samples

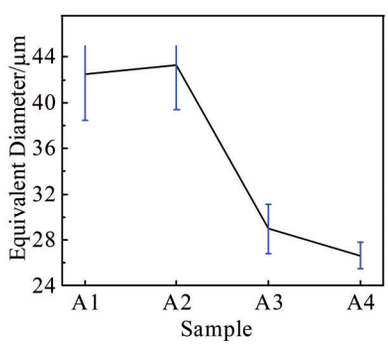

Fig.2 Variation of equivalent grain diameter of α-Al

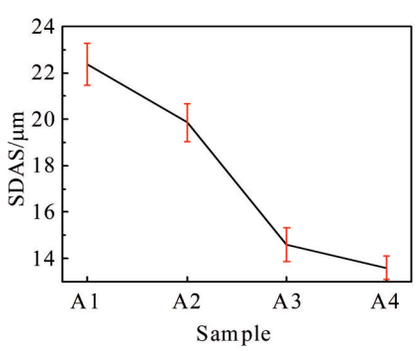

Fig.3 Variation graph of SDAS value

after adding Y element. When Sr coupled with Y was added, the equivalent grain diameter and SDAS value of α-Al reach the minimum, which are 26.63 and 13.60 μm, respectively.

2.2 Morphology of eutectic Si

Fig. 4 is the image of eutectic Si under a high power microscope. It can be seen that the eutectic Si distribution in unmodified A356 alloy is non-directional and irregular, mainly in irregular flake-like or acicular-like with sharp tips, as shown in Fig.4a and 4e. In the sample A2 only added with Sr, there is a clear boundary between α-Al matrix and eutectic Si phase, and eutectic Si is mainly distributed at the grain boundary of α -Al, as shown in Fig. 4b. Moreover, the morphology of eutectic Si changes obviously, the flake-like or acicular-like eutectic Si is interrupted to a great extent and changes into fibrous or short rod-like, as shown in Fig. 4f. Fig. 4c and 4g show that eutectic Si also has a good modification effect after adding Y alone, and most of them are fine fibers, but some of them are blocky. This shows that the modification effect of Y is not as good as that of Sr. When adding Sr coupled with Y into the A356 alloy, the shape and size of α-Al become uniform and fine, the grain boundary of α-Al becomes clearer, and eutectic silicon undergoes obvious modification, as shown in Fig.4d. It can be seen from Fig.4h that the eutectic silicon phase is almost completely transformed into dispersed fine fibers, and the flaky eutectic silicon almost completely disappears.

According to the analysis of above results, Sr has better modification effect on eutectic Si than Y, but has no refinement effect on α-Al grains. Y can not only refine α-Al grains, but also modify eutectic Si, while its modification effect on eutectic Si is not as good as Sr's. When Sr and Y are added together, they have a certain synergistic effect in refining α-Al grains and modifying eutectic Si, which makes the morphology of α-Al grains and eutectic Si reach the best state.

2.3 Element composition and element distribution

Fig. 5a and 5b are the SEM images of sample A1 and A2, respectively, from which we can see that the spots with different contrast are diffusely distributed in the field of view. The element types and contents of each point detected by EDS are shown in Table 3. The results show that the phase with high contrast in Fig. 5a is iron-rich phase, most of which are distributed at the α-Al grain boundary, and a few of them are

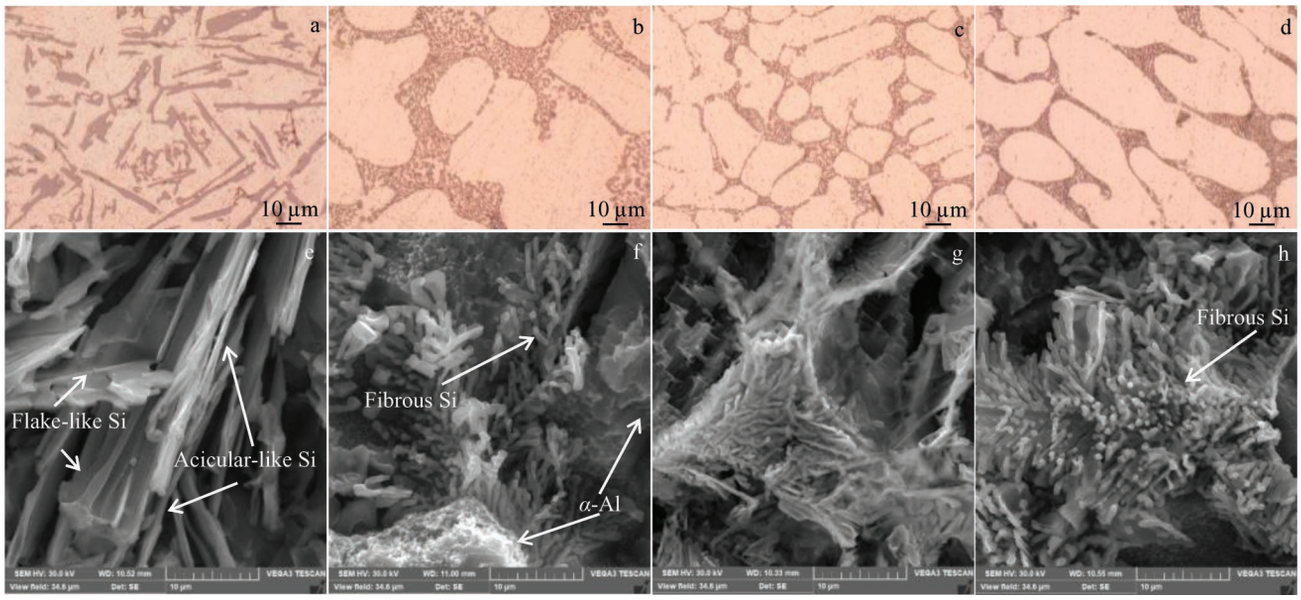

Fig.4 OM morphologies of eutectic Si at high multiple (a~d) and SEM images after deep etching (e~h): (a, e) A1, (b, f) A2, (c, g) A3, and (d, h)

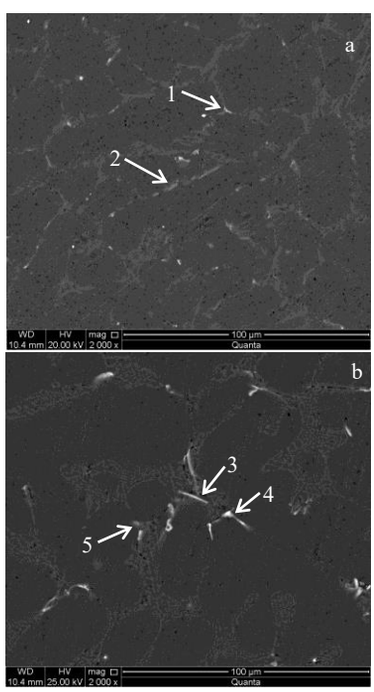

Fig.5 SEM images of sample A1 (a) and A4 (b)

distributed in the α-Al matrix. Two kinds of precipitates with different contrast can be seen in Fig. 5b. The EDS results show that the compounds with the highest contrast are Y-rich compounds, followed by iron-rich phases. These iron-rich phases and Y-rich compounds are distributed at the eutectic site of Al-Si, but almost absent in α-Al matrix.

Fig. 6 shows EDS element mapping of sample A4. It is obvious that Si, Sr and Y elements are mainly distributed in the grain boundaries of α-Al, while Mg element is dispersed in the whole field of view.

Table 3 EDS results of points marked in Fig.5 (wt%)

Point	Al	Si	Mg	Fe	Sr	Y
1	84.79	8.79	1.25	5.17	-	-
2	71.53	17.05	8.38	3.04	-	-
3	89.75	7.87	-	0.04	0.23	2.12
4	70.45	21.70	-	2.00	0.47	5.39
5	98.83	1.08	-	0.09	-	-

2.4 Mechanical properties

2.4.1 Tensile strength and elongation

For A356 aluminum alloy, the strength mainly depends on the grain size of α-Al, while the elongation mainly depends on the morphology of eutectic Si[18].

Fig.7 shows the test results of the mechanical properties of each sample. The tensile strength and elongation of A1 are 166.1 MPa and 3.6%, respectively. When Sr is added alone, the elongation of sample A2 is 6.2%, higher than that of A1, mainly because the eutectic Si is modified by Sr. And then, the morphology changes from plate-like or acicular-like to fibrous shape, which weakens or eliminates the splitting effect of plate-like eutectic Si on the matrix and reduces the tendency of stress concentration at eutectic Si. The elongation of A3 is 6.5% similar to that of A2, but the tensile strength is 184.6 MPa, higher than that of A2. A4 has the highest tensile strength and elongation, i. e. 185.3 MPa and 7.6%, respectively. The main reason is that on the one hand, the addition of Y produces Al_3Y and acts as the heterogeneous nucleation core of α-Al, which increases the nucleation rate and refines the grains of α-Al[19], thus improving the strength; according to the fine grain strengthening theory and Hall-Petch relationship[20]:

$$\sigma_s = \sigma_0 + Kd^{-1/2} \quad (2)$$

it can be seen that the mechanical properties of the alloy increase with the decrease of grain size d. On the other hand,

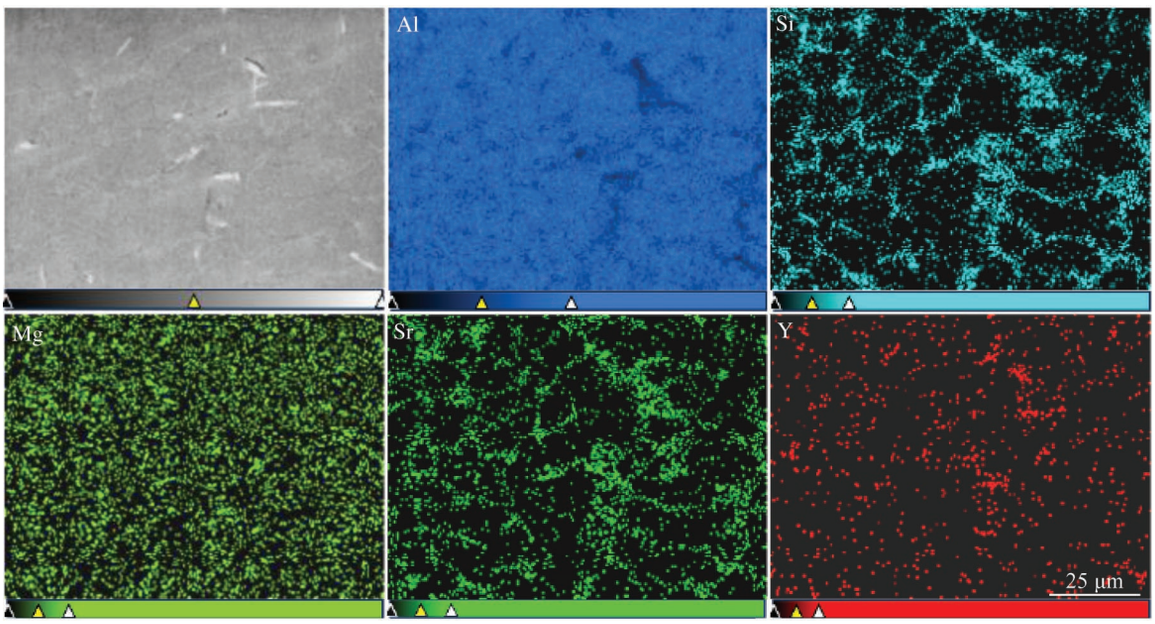

Fig.6 Microstructure and EDS element mappings of sample A4

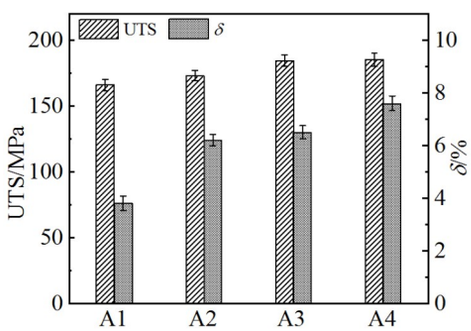

Fig.7 Tensile strength and elongation of sample A1~A4

Y can also modify the eutectic Si[21], the morphology of eutectic Si is improved and the elongation is increased. All of this is consistent with the results of microscopic observation.

2.4.2 Fracture morphology

Fig. 8 shows the tensile fracture morphologies of sample A1~A4, from which we can see that the section of A1 has a large number of dissociation surfaces, which illustrates that the mode of fracture is brittle fracture. With the single addition of Sr or Y or composite addition of Sr and Y, a large number of dimple structures appear on the fracture surface as shown in Fig. 8b~8d. It can be concluded that compared with the remelted A356, the addition of Sr and Y elements modifies eutectic silicon, refines the α-Al grain, increases its elongation, and changes its fracture mode from brittle fracture to ductile-brittle fracture.

3 Grain Refinement Mechanism and Eutectic Si Modification Mechanism

3.1 Refinement mechanism

From the previous analysis, we know that the addition of Y can significantly refine the grain size of α-Al. According to Ref. [9, 22], when Y is added to aluminum alloy, a large number of Al_3Y second phase particles form, which play a role of heterogeneous nucleation in the solidification process of liquid aluminum, so as to improve the nucleation rate and refine the grains. In addition, the radius of Y atom is quite different from that of Al. Y does not exist in the matrix in the form of solid solution, but is enriched at the front of the solid-liquid interface during solidification, resulting in the supercooling of local components in the alloy liquid and the

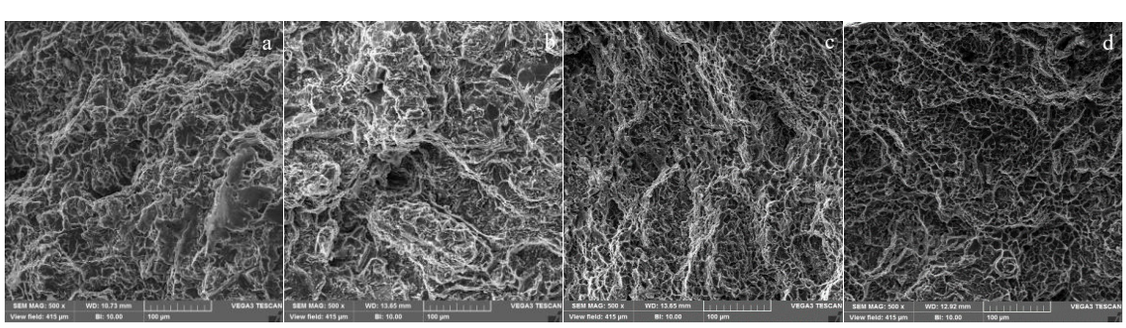

Fig.8 Fracture morphologies of different samples: (a) A1, (b) A2, (c) A3, and (d) A4

refinement of α-Al dendrites.

3.1.1 Mismatch analysis

In the process of heterogeneous nucleation, the smaller the interfacial tension between nucleated solid and substrate, the better the mutual wetting, which is more favorable for nucleation. According to the reason of the interface energy, the more similar the crystal plane structure and the closer the lattice structure, the smaller the interface energy between them. When the crystal plane structure is similar, the mismatch degree of δ is used to represent the coherence between the nucleated solid and the substrate. The two-position mismatch theory and calculation formula are put forward by Bramfitt[23]:

$$\delta_{(hkl)_n}^{(hkl)_s} = \sum_{i=1}^{3} \frac{\left| \left(d_{[uvw]_s} \cos\theta \right) - d_{[uvw]_n} \right|}{\frac{d_{[uvw]_n}}{3}} \times 100\% \quad (3)$$

where $(hkl)_s$ is a low-index plane of the substrate; $[uvw]_s$ is a low-index direction in $(hkl)_s$; $(hkl)_n$ is a low-index plane in the nucleated solid; $[uvw]_n$ is a low-index direction in $(hkl)_n$; $d_{[uvw]_n}$ is the interatomic spacing along $[uvw]_n$; $d_{[uvw]_s}$ is the interatomic spacing along $[uvw]_s$; θ is the angle between the $[uvw]_s$ and $[uvw]_n$.

The smaller the mismatch degree of δ, the better the coherent condition, and the smaller the interfacial tension between the nucleated solid and the substrate, the easier it is for heterogeneous nucleation. It is generally believed that[19] when mismatch δ <6%, it is completely coherent and nucleation is the most effective. When 6%< δ <15%, it is partially coherent, and nucleation is moderately effective. When δ >15%, it is incoherent and the substrate has no heterogeneous nucleation ability.

The lattice types and lattice constants of Al_3Y and α-Al are shown in Table 4, and the calculation results of two-dimensional mismatch are shown in Table 5. Al_3Y is the substrate, and its low index plane is (0001) which is the dense plane. α-Al is the nucleated solid, and its low index plane is (0001) which is also the dense plane, and the atomic distance between the two crystal planes is the closest.

The calculated results show δ=8.19%, which indicates that

Table 4 Lattice types and lattice constants of Al_3Y and α-Al

Eutectic reaction product	Crystal lattice type	Crystal lattice constant/nm
α-Al	fcc	a=0.4049
Al_3Y	Hexagonal	a=0.6195, c=2.1129

Table 5 Calculation of two-dimensional mismatch at the interface of Al_3Y/α-Al

$[uvw]_s$	$[uvw]_n$	$d_{[uvw]_s}$/nm	$d_{[uvw]_n}$/nm	θ/(°)	δ/%	δ/% (average)
$[2\bar{1}\bar{1}0]$	$[10\bar{1}]$	0.6195	0.5726	0	8.19	
$[10\bar{1}0]$	$[11\bar{1}]$	1.073	0.9918	0	8.19	8.19
$[\bar{1}2\bar{1}0]$	$[\bar{1}10]$	0.6195	0.5726	0	8.19	

Al_3Y can be used as a heterogeneous nucleation particle for primary α-Al, and a better heterogeneous nucleation effect can be achieved. Combined with the EDS results (Table 3) and the distribution of Y in the alloy in Fig.6, it is shown that α-Al is based on the Al_3Y formed by the proeutectic reaction for rapid heterogeneous nucleation, which increases the nucleation rate and refines the grains.

3.1.2 Thermal analysis

Fig.9 is the thermal analysis diagram of sample A1~A4. It shows that there are two obvious exothermic peaks during the solidification of A356. Combined with the elements and phases in the alloy, it can be obtained that exothermic peak A and exothermic peak B correspond to two reaction processes of L→α-Al and L→α-Al+Si, respectively. After adding Sr and Y, the initial solidification temperature of α-Al moves to the right compared with that without addition, so that α-Al begins to solidify under a lower undercooling. The single addition of Sr or Y has no effect on the initial temperature of eutectic reaction, but after the composite addition of Sr and Y, the initial temperature of eutectic reaction is about 3.31 °C, lower than that of other three groups of samples, thus increasing the undercooling of eutectic reaction. It can be explained that in the process of eutectic reaction, Sr and Y elements are enriched in front of the solid-liquid boundary, resulting in composition undercooling and promoting the eutectic reaction[24].

3.2 Modification mechanism of eutectic Si

The theories of "impurity-induced twins" (IIT)[25] and "twin plane reentrant edge" (TPRE)[26, 27] are generally accepted. In the study of Xu[28], it is considered that the modification mechanism of Sc on eutectic Si is IIT, and that of Sr on eutectic Si is TPRE. Lu[29] proposed in 1985 that TPRE is the main growth mechanism in Na modified Al-Si alloy. Nafisi[30] proposed that after the eutectic Al nucleates on the primary α-Al dendrites, the Si in the residual solution is enriched to form fine silicon particles at the front of solidification, and flake and fibrous eutectic silicon can form on the particles.

In Al-Si eutectic system, Si phase is solidified by faceted manner. The morphology of unmodified eutectic silicon is plate-like or acicular-like, overlapping each other, and is randomly distributed in the aluminum matrix, as shown in Fig. 4a. The growth characteristics of unmodified eutectic

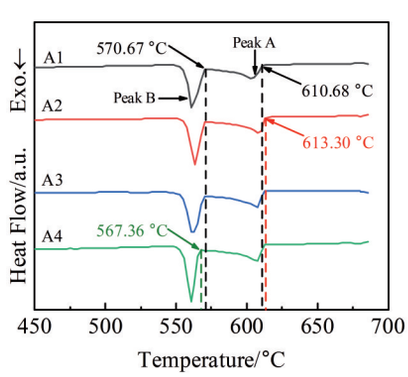

Fig.9 DSC curves of sample A1~A4

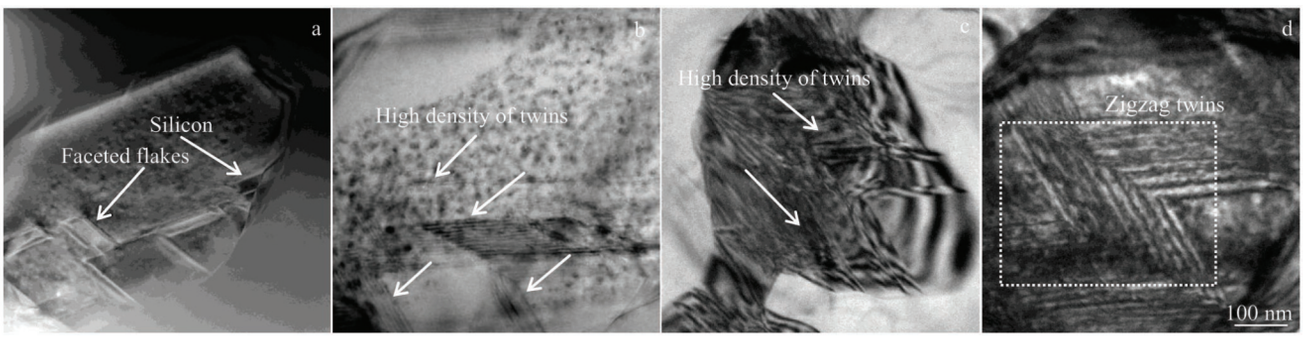

Fig.10 TEM images of different samples: (a) A1, (b) A2, (c) A3, and (d) A4

silicon are faceted silicon flakes as shown in Fig. 10a. These faceted steps on unmodified eutectic silicon are inherent, not accidental or caused by other reasons[25]. The existence of steps contributes to the growth of unmodified eutectic silicon. Therefore, the growth mode of unmodified eutectic silicon belongs to the typical facet step growth.

According to Fig. 10b~10d, high-density twins appear in most eutectic silicon, which provides strong evidence for the mechanism of IIT. The area shown in Fig. 10b~10d is parallel twins with a certain angle, which is due to the large-angle branching caused by the growth of eutectic silicon twins[31]. The modified eutectic silicon shows typical zigzag growth, as shown in Fig. 10d. During the solidification process of Si phase, Sr and Y atoms accumulate in front of the solid-liquid boundary and attach to the single-layer growth step of Si, which interrupts the regular arrangement of Si atoms in the original growth direction, so that the stacking order of Si rows from subsequent diffusion is changed[31]. It also causes Si lattice distortion, increases the energy required for eutectic silicon to grow along the original preferred growth direction and induces twins, which leads to eutectic silicon growing along the [211] direction[14, 32]. In addition, when the eutectic Si grows along a certain direction of the twin plane, the twin grooves always exist, which ensures the continuous growth of the twins, that is the TPRE, and the twins continue to grow in many directions, which leads to the high branching of eutectic silicon and finally the formation of fiber-like structure.

In short, Sr and Y atoms are adsorbed at the front of the solid-liquid interface of eutectic silicon, changing the stacking order of atoms on the surface of the eutectic silicon, thus promoting the IIT. A large number of twins grow in a TPRE mechanism, which suppresses the original growth of eutectic Si and promotes the multi-branching of eutectic silicon and the formation of fiber structure.

4 Conclusions

1) When Sr and Y are added into A356, the optimal equivalent grain diameter (28.97 μm) and secondary dendrite arm spacing (14.59 μm) of α-Al can be obtained. Eutectic Si is completely modified, and its micromorphology changes from plate-like or acicular to fibrous shape. The tensile strength and elongation are increased to 185.3 MPa and 7.6%, respectively.

2) When Sr and Y are added into A356, the grain refinement mechanism is mainly the heterogeneous nucleation of α-Al based on Al_3Y, which accelerates the nucleation rate and refines the grains.

3) When Sr and Y are added into A356, Sr and Y have a similar modification mechanism. Sr and Y as modified atoms accumulate on the edge of the original growth step of eutectic Si to induce twins. The original facet step growth is changed, which is carried out by the mechanism of TPRE.

Reference

1 Fan Songjie, He Guoqiu, Zhang Weihua *et al. Materials Reports*[J], 2007(9): 59 (in Chinese)
2 Wang Zhengjun, Zhang Man, Zhang Qiuyang *et al. Rare Metal Materials and Engineering*[J], 2020, 49(10): 3402 (in Chinese)
3 Yi H E, Xi H H, Ming W Q *et al. Transactions of Nonferrous Metals Society of China*[J], 2021, 31(1): 1
4 Zhang Jiahong, Xing Mingshu. *Materials Reports*[J], 2018, 32(11): 1870
5 Wang Q G. *Metallurgical Materials Transactions A*[J], 2003, 34(12): 2887
6 Gan Junqi, Huang Yujian, Wen Cheng *et al. Transactions of Nonferrous Metals Society of China*[J], 2020, 30(11): 2879
7 Timpel M, Wanderka N, Schlesiger R *et al. Acta Materialia*[J], 2012, 60(9): 3920
8 Gursoy O, Timelli G. *Journal of Materials Research Technology*[J], 2020, 9(4): 8652
9 Mao Guoling, Yan Han, Zhu Congcong *et al. Journal of Alloys and Compounds*[J], 2019, 806: 909
10 Mazahery A, Shabani M O. *JOM*[J], 2014, 66(5): 726
11 Marco Colombo A, Elisabetta Gariboldi A, Alessandro Morri B. *Journal of Alloys and Compounds*[J], 2017, 708: 1234
12 Chen Zhiqiang, Jia Jinyu, Hu Wenxin *et al. Rare Metal Materials and Engineering*[J], 2020, 49(10): 3388 (in Chinese)
13 Liu W, Xiao W, Cong X *et al. Materials Science Engineering A*[J], 2017, 693: 93
14 Qiu C, Miao S, Li X *et al. Materials Design*[J], 2017, 114(1): 563
15 Dong Y, Zheng R, Lin X *et al. Journal of Rare Earths*[J], 2013,

31(2): 204
16 Nogita K, Drennan J, Dahle A *et al. Materials Transactions*[J], 2005, 44(4): 625
17 Yang C L, Li Y B, Dang B *et al. Transactions of Nonferrous Metals Society of China*[J], 2015, 25(10): 3189
18 Fang Qiu, Xiao Yun. *China Foundry*[J], 2014, 11(4): 287
19 Liu Zheng, Chen Qingchun, Guo Song *et al. Rare Metal Materials and Engineering*[J], 2015, 44(4): 859 (in Chinese)
20 Liao H, Zhan M, Li C *et al. Journal of Magnesium Alloys*[J], 2020, 9(4): 1215
21 Wei Z, Lei Y, Yan H *et al. Journal of Rare Earths*[J], 2019, 37(6): 103
22 Hu X P, Wang Q, Hu H *et al. Rare Metals*[J], 2021, 40(11): 10
23 Bramfitt B L. *Metallurgical Transactions*[J], 1970, 1(7): 1987
24 Heiberg G, Nogita K, Dahle A K *et al. Acta Materialia*[J], 2002, 50(10): 2537
25 Lu S Z, Hellawell A. *Metallurgical Transactions A*[J], 1987, 18(10): 1721
26 Wagner R S. *Acta Metall Sin*[J], 1960, 8(1): 57
27 Hamilton D R, Seidensticker R G. *Journal of Applied Physics*[J], 1960, 31(7): 1165
28 Xu C, Wang F, Mudassar H *et al. Journal of Materials Engineering & Performance*[J], 2017, 26(4): 1605
29 Lu S Z, Hellawell A. *Journal of Crystal Growth*[J], 1985, 73(2): 316
30 Nafisi S, Ghomashchi R, Vali H. *Materials Characterization*[J], 2008, 59(10): 1466
31 Zheng Qiuju, Zhang Lili, Jiang Hongxiang *et al. Journal of Materials Science & Technology*[J], 2020, 47(12): 142
32 Li J H, Barrirero J, Engstler M *et al. Metallurgical Materials Transactions A*[J], 2015, 46(3): 1300

Sr和Y添加对A356铝合金显微组织和力学性能的影响及机理

张艺杰[1]，杜景红[1]，吉全鑫[1]，孙彦华[2]，冯伟光[2]，包崇军[2]，李玉章[2]，严继康[3]
(1. 昆明理工大学 材料科学与工程学院，云南 昆明 650093)
(2. 昆明冶金研究院有限公司，云南 昆明 650031)
(3. 西南石油大学 工程学院，四川 南充 637001)

摘　要：通过金相显微镜、扫描电镜、透射电镜观察，能谱分析以及力学性能实验，研究了添加Sr和Y对A356铝合金显微组织和力学性能的影响。结果表明，相比于单加Sr或Y，复合添加Sr和Y时，共晶Si由板片状或针状完全转变为纤维状，α-Al的等效晶粒直径从42.49 μm减小至26.63 μm，二次枝晶臂间距从22.38 μm减小至13.60 μm，抗拉强度从166.1 MPa增加到185.3 MPa，延伸率从3.6%提高至7.6%，断裂方式也从脆性断裂转变为韧脆型断裂。探讨了Sr和Y复合添加时的细化机理和变质机理，得出α-Al晶粒细化的主要原因是α-Al以Al_3Y为基底进行快速非均质形核，变质机理为杂质诱导孪晶并以孪晶凹谷机制进行生长。

关键词：A356；晶粒细化；共晶Si变质；错配度；孪晶

作者简介：张艺杰，男，1995年生，硕士，昆明理工大学材料科学与工程学院，云南 昆明 650093，E-mail：577645651@qq.com